

Accepted Manuscript

Discovery of 1,8-acridinedione derivatives as novel GCN5 inhibitors via high throughput screening

Huan Xiong, Jie Han, Jun Wang, Wenchao Lu, Chen Wang, Yu Chen, Fulin Lian, Naixia Zhang, Yu-Chih Liu, Chenhua Zhang, Hong Ding, Hualiang Jiang, Wencong Lu, Cheng Luo, Bing Zhou

PII: S0223-5234(18)30127-2

DOI: [10.1016/j.ejmech.2018.02.005](https://doi.org/10.1016/j.ejmech.2018.02.005)

Reference: EJMECH 10182

To appear in: *European Journal of Medicinal Chemistry*

Received Date: 6 January 2018

Revised Date: 31 January 2018

Accepted Date: 3 February 2018

Please cite this article as: H. Xiong, J. Han, J. Wang, W. Lu, C. Wang, Y. Chen, Fulin Lian, N. Zhang, Y.-C. Liu, C. Zhang, H. Ding, H. Jiang, W. Lu, C. Luo, B. Zhou, Discovery of 1,8-acridinedione derivatives as novel GCN5 inhibitors via high throughput screening, *European Journal of Medicinal Chemistry* (2018), doi: 10.1016/j.ejmech.2018.02.005.

This is a PDF file of an unedited manuscript that has been accepted for publication. As a service to our customers we are providing this early version of the manuscript. The manuscript will undergo copyediting, typesetting, and review of the resulting proof before it is published in its final form. Please note that during the production process errors may be discovered which could affect the content, and all legal disclaimers that apply to the journal pertain.



Discovery of 1,8-acridinedione derivatives as novel GCN5 inhibitors via high throughput screening

Huan Xiong^{a,b,#}, Jie Han^{c,e,#}, Jun Wang^{c,d,#}, Wenchao Lu^{c,e}, Chen Wang^{c,e}, Yu Chen^{c,e}, Fulin Lian^c, Naixia Zhang^c, Yu-Chih Liu^f, Chenhua Zhang^f, Hong Ding^c, Hualiang Jiang^c, Wencong Lu^{a,*}, Cheng Luo^{c,e,*}, and Bing Zhou^{b,*}

^aDepartment of Chemistry, College of Sciences, Shanghai University, 99 Shangda Road, Shanghai 200444, China

^bDepartment of Medicinal Chemistry, Shanghai Institute of Materia Medica, Chinese Academy of Sciences, 555 Zuchongzhi Road, Shanghai 201203, China

^cCAS Key Laboratory of Receptor Research, State Key Laboratory of Drug Research, Shanghai Institute of Materia Medica, Chinese Academy of Sciences, 555 Zuchongzhi Road, Shanghai 201203, China

^dJiangsu Key Laboratory for High Technology Research of TCM Formulae, Nanjing University of Chinese Medicine, 138 Xianlin Road, Nanjing 210023, China

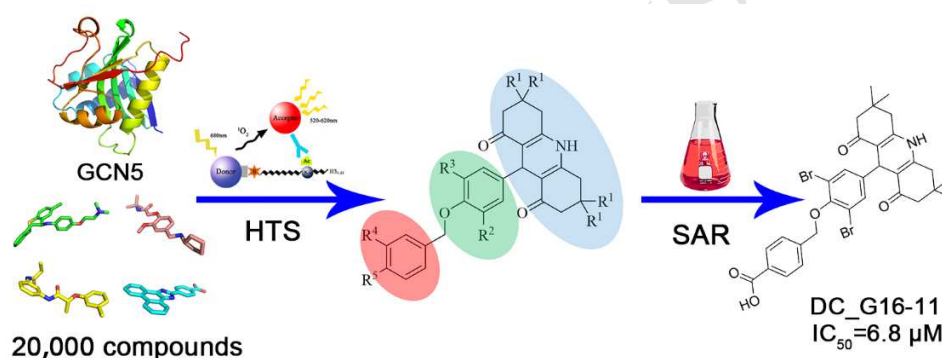
^eUniversity of Chinese Academy of Sciences, 19 Yuquan Road, Beijing 100049, China

^fIn Vitro Biology, Shanghai ChemPartner Life Science Co., Ltd., #5 Building, 998 Halei Road, Shanghai 201203, China

* Corresponding authors.

These authors contributed equally.

ABSTRACT: The general control nonrepressed protein 5 (GCN5) plays a crucial role in many biological processes. Dysregulation of GCN5 has been closely related to various human diseases, especially cancers. Hence, the exploitation of small molecules targeting GCN5 is essential for drug design and academic research. Based on the amplified luminescent proximity homogeneous assay screen methodology, we performed high throughput screening and discovered a novel GCN5 inhibitor **DC_G16** with 1,8-acridinedione scaffold. Structure optimization led to the identification of a highly potent inhibitor, namely **DC_G16-11** with the half-maximal inhibitory concentration (IC_{50}) value of 6.8 μM . The binding between **DC_G16-11** and GCN5 was demonstrated by NMR and SPR with a K_D of 4.2 μM . It could also inhibit proliferation and induce cell cycle arrest and apoptosis in cancer cells while it presented minimal effects on normal cells. Herein, **DC_G16-11** could be applied as a validated chemical probe for GCN5-related biological function research and presented great potential for clinical disease treatment.



Highlights

- A potent GCN5 inhibitor with a new scaffold was identified via high throughput screening.
- The direct binding interactions between compounds and GCN5 were demonstrated by NMR and SPR.
- Further chemical optimization led to the identification of **DC_G16-11** with improved activity *in vitro*.
- The detailed binding mode between **DC_G16-11** and GCN5 and structure-activity relationship was disclosed by molecular docking.

Keywords

Epigenetics; Histone acetyltransferase; GCN5; High throughput screening; 1,8-acridinedione derivative

1. Introduction

Histone acetylation, one of the most important post-translational modifications in epigenetics, plays a vital role in chromatin remodeling and gene transcription [1, 2]. The acetylation level of histones is altered by the synergy effects of histone acetyltransferases and deacetylases. Dysfunction of them leads to aberrant cellular processes and multiple diseases [3, 4]. The general control nonrepressed protein 5 (GCN5), originally identified in yeast, shows a preference for H3K14, while it can also acetylate H3K8 and H4K16 to a weaker extent [5-7]. Besides histones, many transcription factors can be also acetylated by GCN5 such as p53 and PGC-1 α [8, 9]. Many studies show that GCN5 is a critical regulator in cell cycle and metabolic processes, which is closely related to cancer progression and metabolic disorders [10-12]. GCN5 expression is elevated in colon cancer and inhibition of GCN5 blocks the proliferation of colon cancer cells [13]. Overexpression of transcription factors such as E2F1 was tightly regulated by GCN5 in non-small-cell lung cancer [14]. GCN5 also takes part in the activation of the oncogenic EGF signaling pathway in many cancer subtypes [15]. In leukemic cells, GCN5 acetylates and stabilizes chimeric transcription factor E2A-PBX1, which contributes to cell transformation [16]. Collectively, the oncogenic role of GCN5 has been evidenced in the literature making it an attractive therapeutic target for chemical intervention.

Several HAT inhibitors with different scaffolds have been reported and generally, they can be classified as bi-substrate inhibitors, natural products and synthetic compounds. Bi-substrate inhibitors are synthesized peptide CoA conjugates. In 2002, Poux and colleagues developed the H3-(Me)CoA-20 as the potent inhibitor for tetrahymena GCN5 with the IC₅₀ value of 500 nM [17]. However, the lack of stabilization and cell permeability of bi-substrate inhibitors limit their further development in drug design [18]. Natural products such as garcinol and anacardic acid have been reported to decrease the acetylation level in a variety of cell models [19]. Nonetheless, due to their polypharmacology effects at cellular level, it's difficult to clarify the precise mechanism of action of natural products [20]. Synthetic compounds have unique advantages of significantly low production cost and easy drug delivery. Hence, many synthesized small molecules were developed as GCN5 inhibitors. γ -Butyrolactone MB-3 is the first reported small-molecule inhibitor of GCN5 with IC₅₀ value of 100 μ M [21]. Isothiazolone and its derivatives were identified as pan-HAT inhibitors that presented broad inhibition of HATs [22, 23]. Although many of these compounds have been developed to underscore the therapeutic potential for HATs, none of them has entered into clinic trials. Recently, many breakthroughs have been made in the development of small molecular inhibitors for p300 [24, 25]. Instead, the researches on GCN5 inhibitors still lag behind. Therefore, the exploitation of potent and selective GCN5 inhibitors with novel scaffolds is essential for drug design in GCN5-related mechanism studies.

Herein, we identified a novel GCN5 inhibitor **DC_G16** via high throughput screening based on the amplified luminescent proximity homogeneous assay. The inhibitory activity of **DC_G16** was validated by radioactive acetylation assay. Both SPR and NMR studies gave convincing evidence of the direct binding between GCN5 and **DC_G16**. The design and optimization based on that scaffold resulted in the discovery of **DC_G16-11** with improved potency *in vitro*. Molecular docking studies proposed that **DC_G16-11** occupied the pocket of H3 substrate in a competitive manner. Further studies at cellular level showed that **DC_G16-11** reduced the acetylation in H3K14 and inhibited cell growth in MV4-11 cell lines while it presented minimal effects on normal cells supporting its potential use for clinical translation.

2. Results and Discussion

2.1 Discovery of hit compound DC_G16 through HTS

Nowadays, high throughput screening has developed rapidly and becomes a powerful tool for pharmaceutical research in both academia and industry [26]. The ALPHAScreen is an efficient and reliable method for studies in enzyme kinetics and protein-protein interactions and has been widely applied in epigenetic-related research [27]. In this study, a high throughput screening platform based on ALPHAScreen assay was established to screen in-house compound library containing about 20,000 diverse compound collections (**Figure S1**). As shown in **Figure 1a**, the primary screening was carried out at concentration of 100 μM . The compounds with inhibition rate higher than 70% at 100 μM were selected for further validation. The remaining 47 hit compounds were re-purchased and re-tested in a dose-dependent assay leading to the identification of eight candidate compounds with significant dose-dependent inhibitory activity for GCN5. Then, in order to rule out the possibility of false positives commonly observed in ALPHAScreen assays, radioactive acetylation assays were performed to validate the compounds' inhibitory activity. Among them, DC_G18, DC_G31, DC_G7, DC_G16 and DC_G11 presented inhibitory activity with IC_{50} value of 2.9 μM , 20.0 μM , 8.6 μM , 34.7 μM and 19.0 μM , respectively and were kept for follow-up NMR studies (**Figure 1b**, **Figure 2a**). Both Carr-Purcell-Meiboom-Gill (CPMG) and saturation transfer difference (STD) in NMR studies revealed that only **DC_G16** could bind to the catalytic domain of GCN5 (**Figure 2b**, **2c**). The direct binding between **DC_G16** and GCN5 was further measured quantitatively using SPR with a K_D value of 26.2 μM (**Figure 2d**), which was in accordance with the inhibitory activity in radioactive acetylation assay (**Figure 2a**). Hence, we identified **DC_G16** as a hit compound for follow-up optimization.

2.2. Chemistry

2.2.1. Synthesis

A series of derivatives were designed and synthesized for structure optimization based on **DC_G16**. The synthetic routes employed to prepare the new derivatives **6a-6h** are depicted in **Scheme 1** and **Scheme 2**. The key intermediates **4a-4e** were prepared through a modified Hantzsch reaction. Condensation of 1,3-cyclohexanedione (**1a**) / dimedone (**1b**) with corresponding aromatic aldehydes (**2a-2e**) and ammonium acetate (**3**) in the presence of ionic liquid in anhydrous ethanol afforded the desired intermediates **4a-4e** in acceptable yields. The ionic liquid was prepared according to the literature procedure [28]. In the next step, advanced intermediates **4a-4e** and **4f** were reacted with **5a-5c** in the presence of potassium hydroxide in anhydrous DMSO to obtain the target compounds **6a-6h**. The synthetic route for the preparation of the target compounds **9a-9c** is illustrated in **Scheme 3**. The synthesis of key intermediates **8a-8b** was carried out by treatment of 4-hydroxybenzaldehyde and 1,3-cyclohexanedione dissolved in dry THF with appropriate amine in the presence of piperidine, according to the literature [28]. The synthesis of the intermediate **8c** via one-pot multicomponent condensation of 1,3-cyclohexanedione, α -naphthylamine and 4-hydroxybenzaldehyde in butanol is shown in **Scheme 2** [29]. Intermediates **8a-8c** were further derivatized by a similar procedure as described above with 4-(bromomethyl)benzoic acid to give the target compounds **9a-9c**.

2.2.2. Structure-activity relationship studies and selectivity profiling

For the convenience of description, we divided the general scaffold into three parts: H, M and T, referred to head, middle and tail regions, respectively (**Figure 3a**). With the hit compound (**6a**) in hand, a series of derivatives were obtained by chemical synthesis and tested (**Table 1**) to get a deeper understanding of the structure activity relationship (SAR). Firstly, replacement of the dichloro group in the M region (R^2 and R^3) with the methoxy group and hydrogen in the compound **6b** led to decrease of its inhibitory activity

(Table 1, entry 2) indicating the essential role of halogen atoms in the M region in the compounds. Therefore, with the R² and R³ in the M region substituted with one halogen group, we conducted slight modification on 1,3-cyclohexanedione to make T region more hydrophobic. Intriguingly, the resulting compound **6c** performed a little improved inhibitory activity (Table 1, entry 3) than **6a**. Encouraged by the result, we initiated a couple of changes in the T region to explore whether the number of rings in the T region restrict compounds activity. Bicyclic derivatives **9a** and **9b**, and tetracyclic derivative **9c** were synthesized as illustrated in Scheme 2 and showed similar weak activity (Table 1, entry 4-6). Combined with the inhibitory activity of the intermediates **6h** and **4c** (Table 1, entry 7, 8), we concluded that both H and T regions were important for GCN5 inhibitory activity. To further investigate the SAR in H region, we found that replacement of the carboxyl group (R⁵) by hydrogen (**6d**) and addition of fluorine as R⁴ (**6e**) led to a significant decrease in their inhibitory activity which underlined the importance of carboxyl group (Table 1, entry 9,10). Taken together, we retained substituent groups based on the structure of **6c** and add another bromo group as R² to obtain the compound **6f** (DC_G16-11) (Table 1, entry 11). **6f** exhibited more than 5-fold increase in inhibitory activity versus **6a** with an IC₅₀ value of 6.8 μM (Figure 3b). Meanwhile, **6f** presented good selectivity against p300, EZH2 and G9a with inhibition rate of 21%, 7% and -8% at 33 μM. Taken together, **6f** and the negative compound **6e** were selected for further evaluation.

2.3. Binding assay based on SPR

Given the prominent potency of DC_G16-11, surface plasmon resonance (SPR) based binding assay was performed to quantitatively determine the binding affinity between DC_G16-11 and GCN5. The results demonstrated the binding between DC_G16-11 and GCN5 with a K_D value of 4.2 μM (Figure 4a). Compared with DC_G16, DC_G16-11 presented a higher binding affinity with GCN5, which was consistent with inhibitory activity measured by radioisotope assays.

2.4. Binding mode analysis

To further disclose the molecular mechanism of inhibitory activity of DC_G16-11, we employed molecular docking studies to investigate the binding mode between GCN5 and the inhibitors. A putative binding pose of DC_G16-11 was generated using Glide program with XP mode. The results revealed that DC_G16-11 occupied the substrate H3 peptide pocket in GCN5 which may account for its *in vitro* activity (Figure 4b). The carboxyl group in the H region formed a hydrogen bond to the carbonyl group of Y212 which clearly explained the differences in inhibitory activity between DC_G16-11, **6e** and **6d**. The lack of carboxyl group in **6e** and **6d** significantly diminished GCN5 inhibition activity as is presented in Table 1. In addition, another two hydrogen bonds were observed between DC_G16-11 and the sidechain of K242, Y135 in GCN5 catalytic pocket (Figure 4c). Besides polar interactions, a hydrophobic environment surrounded by V175, F176, Y244, Y212, Y240 and Y135 stabilized the DC_G16-11 conformations in pocket (Figure 4c). The main difference between DC_G16 and DC_G16-11 in the substitution of Br instead of Cl unexpectedly improved the activity of compound. An assumption was proposed that the halogen bond [30] was formed between E173, the most important catalytic residue in GCN5, and halogen in M region with $d(\text{Br}\cdots\text{O}) = 2.9 \text{ \AA}$ and $\angle(\text{C}-\text{Br}\cdots\text{O}) = 130^\circ$. The intensity of Br \cdots O is stronger than Cl \cdots O, which may explain the improvement in inhibitory activity from DC_G16 to DC_G16-11.

2.5. Cell-based assays

To explore the cellular activity of **DC_G16-11** in cancer cells, we measured cell viability of MV4-11 leukemia cells for 3 days by CellTiter-Glo luminescent assays. The results showed that **DC_G16-11** could induce a dose-dependent cell growth inhibition with the IC_{50} value of 24.7 μ M which presented minimal effect on HUV-EC-C and MRC5 normal cells growth (**Figure 5a, Figure S3**). As expected, the negative compound **6e** could not retard the proliferation of MV4-11 (**Figure S2a**). Then western blot assay was conducted to evaluate the acetylation patterns in MV4-11. The results showed that the acetylation level of H3K14 was significantly reduced by treatment of **DC_G16-11** for 24 h compared to negative control compound **6e** (**Figure 5b, Figure S2b**), which demonstrated the on-target behavior of **DC_G16-11**. Additionally, treatment of **DC_G16-11** could significantly led to cell cycle arrest in G0/G1 phase and induced apoptosis in a dose-dependent manner in MV4-11 cells (**Figure 5c-d**).

3. Conclusion

Acetyltransferase, which transfers acetyl from Ac-CoA to histone and non-histone substrates, has been considered as a significant regulatory factor in epigenetic modification. GCN5, one of the members in GNAT subfamily, has got more and more attention for its global acetylation activity. However, in stark contrast to p300/CBP, the development of the selective GCN5 inhibitor has progressed quite slowly. In this study, we identified **DC_G16** as a potential GCN5 inhibitor by ALPHAScreen-based high throughput screening. Radioactive acetylation assays confirmed the inhibitory activity with an IC_{50} value of 34.7 μ M. Biophysical methods including NMR and SPR demonstrated the direct binding between **DC_G16** and GCN5. Based on the scaffold, a series of derivatives were designed and synthesized to evaluate their inhibition activity. Among them, **DC_G16-11** presented the best inhibitory activity against GCN5 with an IC_{50} value of 6.8 μ M. The binding affinity was also validated by SPR with a K_D value of 4.2 μ M. Further molecular docking studies proposed that **DC_G16-11** occupied substrate H3 pocket which accounted for its inhibitory activity *in vitro* and provided atomic-resolution interpretation of structure activity relationship. On the cellular level, **DC_G16-11** could retard the proliferation of MV4-11 cell lines while it showed no effects on normal cells. Meanwhile, the treatment of **DC_G16-11** reduced the acetylation level on H3K14 and led to cell cycle arrest and apoptosis, which validated the biological activity of this new scaffold compounds in leukemic models. Taken together, **DC_G16-11** represents the novel scaffold which deserves further structure optimization and lays a solid foundation for future drug design and GCN5-related mechanism studies.

4. Method

4.1. Plasmid construction, protein expression and purification

Sequence encoding the HAT domain of yeast GCN5 (residues 99-262) was cloned in pRSET vector and transformed into Escherichia coli BL21 (DE3). The cells were grown in LB medium at 37 °C for 4-6 h until the OD_{600} reached 0.8. Cells were induced by adding 0.5 mM isopropyl β -D-1-thiogalactopyranoside and cultured overnight at 16 °C before harvest by centrifugation. Cell pellets were re-suspended and lysed in lysis buffer (50 mM HEPES pH 8.0, 500 mM NaCl and 20 mM imidazole) followed by centrifugation at 18,000 rpm. Then supernatant was loaded onto HisTrap FF column (GE Healthcare). The protein was eluted from the column with an increasing concentration of imidazole in lysis buffer (20-500 mM) and further purified by SP FF column cation-exchange (GE Healthcare) and Superdex200 column (GE Healthcare) in final buffer containing 20 mM HEPES (pH 8.0), 150 mM NaCl, 1 mM DTT. The purified protein was concentrated to 10 mg/mL and flash-frozen in liquid nitrogen for further experiments.

4.2. High throughput screening based on amplified luminescent proximity homogeneous assay

In order to discover potential GCN5 inhibitors, high throughput screening was performed based on amplified luminescent proximity homogeneous assay. Compounds from in house compound library were diluted and incubated with 5 nM protein in optimized assay buffer for 30 min in 384-well plate. Then 2 μ M AC-CoA and 100 nM H3 peptide (1-23) tagged with biotin were added and reacted for 30 min at room temperature. Subsequently, the detection reagent comprising of acceptors beads coupled with anti-H3K14AC and donor beads was transferred to the assay plate. The whole system was incubated for 60 min at room temperature before amplified chemiluminescent signal at 570 nm was collected on the multilabel reader. All data were analyzed in Graphpad Prism 6.0. Detailed information about high throughput screening and assay development is provided in Supplementary material (**Table S1, Figure S1**).

4.3. Radioactive acetylation assay

Briefly, the compounds in a range of concentrations were pre-incubated with protein for 15 min and added to reactions containing peptide and [3 H]-Ac-CoA in optimized Tris buffer. Subsequently, 25 μ L of the mix solution per well was transferred to Flashplate from assay plate. After 60 min of incubation at 37°C, reaction was stopped by cold Ac-CoA. Then the whole reaction system was read on Microbeta. The data was analyzed by GraphPad Prism 6.0 to obtain IC₅₀ values.

4.4. NMR assay

The interaction between compounds and yGCN5 was investigated by a Carr-Purcell-Meiboom-Gill (CPMG) and saturation transfer difference (STD) experiments as described before [31]. Compounds and yGCN5 protein were diluted to 200 μ M and 5 μ M, respectively, in assay buffer (20 mM NaH₂PO₄, 20 mM Na₂HPO₄, 100 mM NaCl, pH 7.4) containing 5% DMSO. All NMR assays were carried out on 600 MHz Bruker Avance III spectrometer with a cryo-probe (Bruker Biospin, Germany).

The solvent-suppressed 1D-¹H CPMG (cpmgPr1d) was acquired by [RD-90°-(τ -180°- τ)n-ACQ] pulse sequence. A 54.78 dB pulse during the recycle delay (RD) of 4 s was employed to avoid water resonance. 90° pulse length was adjusted to around 11.82 μ s. Finally, we collected 4 dummy scans and 64 free induction decays (FID) into 64K acquisition point with a spectral width of 12 KHz (20 ppm) and an acquisition time (AQT) of 2.73 s. 128 scans in totally 20 min acquisition time were used in STD experiment including the acquisition time of 1.71 s, 4 dummy scans, relaxation delay of 3 s and a 40 dB pulse with the irradiation frequency at 0.25 ppm or -1000 ppm, alternatively.

4.5. Surface Plasmon Resonance (SPR) based binding assay

The SPR binding assays were performed on a Biacore T200 instrument (GE Healthcare). GCN5 protein was covalently coupled on CM5 chip according to standard procedure [32]. The whole system was equilibrated overnight first with HBS buffer (20 mM HEPES (pH 7.4), 150 mM NaCl, 0.05% (v/v) surfactant P20, and 0.25% (v/v) dimethyl sulfoxide). Compounds were diluted with HBS buffer and then injected at a flow of 30 μ L/min for 60 s to contact, followed by disassociation for 300 s. The equilibrium dissociation constants of the compounds were determined by Biacore T200 evaluation software (GE Healthcare).

4.6. Chemistry

All solvents were purchased from commercially available sources and used without purification (HPLC or analytical grade). Anhydrous solvents were purchased from Sigma-Aldrich and stored under nitrogen

atmosphere with activated molecular sieves. All reagents were purchased from Sigma Aldrich and Alfa Aesar and used without further purification, unless otherwise indicated. All products were characterized by their NMR and MS spectra. ¹H NMR and ¹³C NMR spectra were obtained on Bruker Avance 400 or 500 instruments at 400/100 MHz or 500/125 MHz, respectively. Chemical shifts were reported in parts per million (ppm, δ) downfield from tetramethylsilane (TMS) as the internal standard and coupling constants (*J* values) were reported in Hertz (Hz). Proton coupling patterns were described as broad (b), singlet (s), doublet (d), triplet (t), quartet (q), multiplet (m). Reactions were monitored by thin-layer chromatography or UPLC-MS analysis. Column chromatography (petroleum ether/ethyl acetate) was performed on silica gel (200-300 mesh). Yields were not optimized.

4.6.1. General procedure A for synthesis of 1,8-acridinedione intermediates 4a-4e

The catalyst ionic liquid was prepared according to the literature procedure [28]. To a mixture of 1,3-cyclohexanedione/dimedone (2 mmol), arylaldehyde (1 mmol), and ammonium acetate (3 mmol) in 5 mL of anhydrous ethanol, and 0.02 g of ionic liquid was added and stirred at 80°C for 4 h. After completion of the reaction (TLC monitoring), the mixture was cooled to room temperature. The resulting precipitate was filtered off and washed with ethanol before drying to afford the pure 1,8-acridinedione intermediates in good yields (50-80%) which were submitted to the following step without further purification [33].

4.6.1.1. 9-(3,5-Dichloro-4-hydroxyphenyl)-3,4,6,7,9,10-hexahydroacridine-1,8(2H,5H)-dione (4a)

Compound **4a** was prepared using 3,5-dichloro-4-hydroxybenzaldehyde (191 mg, 1 mmol, 1.0 eq), 1,3-cyclohexanedione (224 mg, 2 mmol, 2.0 eq) and ammonium acetate (231 mg, 3 mmol, 3.0 eq) according to the general procedure A to give the desired product (240 mg, yield 63.5%) as an offwhite solid. ¹H NMR (400 MHz, DMSO-*d*₆) δ 9.52 (s, 1H), 7.01 (s, 2H), 4.77 (s, 1H), 2.56-2.43 (m, 4H), 2.25-2.17 (m, 4H), 1.96-1.86 (m, 2H), 1.85-1.72 (m, 2H). One NH was not seen.

4.6.1.2. 9-(4-Hydroxy-3-methoxyphenyl)-3,4,6,7,9,10-hexahydroacridine-1,8(2H,5H)-dione (4b)

Compound **4b** was prepared using 4-hydroxy-3-methoxybenzaldehyde (152 mg, 1 mmol, 1.0 eq), 1,3-cyclohexanedione (224 mg, 2 mmol, 2.0 eq) and ammonium acetate (231 mg, 3 mmol, 3.0 eq) according to the general procedure A to give the desired product (245 mg, yield 72.3%) as an off-white solid. ¹H NMR (400 MHz, DMSO-*d*₆) δ 9.39 (s, 1H), 8.57 (s, 1H), 6.74 (d, *J* = 1.8 Hz, 1H), 6.55 (d, *J* = 8.1 Hz, 1H), 6.46 (dd, *J* = 8.1, 1.8 Hz, 1H), 4.83 (s, 1H), 3.67 (s, 3H), 2.57-2.42 (m, 4H), 2.26-2.15 (m, 4H), 1.96-1.86 (m, 2H), 1.85-1.72 (m, 2H).

4.6.1.3

9-(3-Bromo-4-hydroxyphenyl)-3,3,6,6-tetramethyl-3,4,6,7,9,10-hexahydroacridine-1,8(2H,5H)-dione (4c)

Compound **4c** was prepared using 3-bromo-4-hydroxybenzaldehyde (201 mg, 1 mmol, 1.0 eq), 5,5-dimethyl-1,3-cyclohexanedione (280 mg, 2 mmol, 2.0 eq) and ammonium acetate (231 mg, 3 mmol, 3.0 eq) according to the general procedure A to give the desired product (370 mg, yield 83.3%) as a light-yellow solid. ¹H NMR (400 MHz, DMSO-*d*₆) δ 9.29 (s, 1H), 7.18 (d, *J* = 2.1 Hz, 1H), 6.92 (dd, *J* = 8.3, 2.1 Hz, 1H), 6.74 (d, *J* = 8.3 Hz, 1H), 4.67 (s, 1H), 4.36 (s, 1H), 2.44 (d, *J* = 17.0 Hz, 2H), 2.31 (d, *J* = 17.0 Hz, 2H), 2.17 (d, *J* = 16.1 Hz, 2H), 1.99 (d, *J* = 16.1 Hz, 2H), 1.00 (s, 6H), 0.88 (s, 6H); ¹³C NMR (126 MHz, DMSO) δ 194.39, 151.69, 149.20, 139.63, 131.72, 127.69, 115.66, 111.30, 108.30, 50.21, 32.16, 31.81, 29.10, 26.39; UPLC-MS *m/z* (ESI, positive) found [M+H]⁺ 444.33, >99% pure.

4.6.1.4. 9-(3-Bromo-4-hydroxyphenyl)-3, 4,6,7,9,10-hexahydroacridine-1,8(2H,5H)-dione (**4d**)

Compound **4d** was prepared using 3-bromo-4-hydroxybenzaldehyde (201 mg, 1 mmol, 1.0 eq), 1,3-cyclohexanedione (224 mg, 2 mmol, 2.0 eq) and ammonium acetate (231 mg, 3 mmol, 3.0 eq) according to the general procedure A to give the desired product (331 mg, yield 85.3%) as an off-white solid. ¹H NMR (400 MHz, DMSO-*d*₆) δ 9.87 (s, 1H), 9.45 (s, 1H), 7.18 (d, *J* = 2.1 Hz, 1H), 6.90 (dd, *J* = 8.3, 2.1 Hz, 1H), 6.75 (d, *J* = 8.3 Hz, 1H), 4.77 (s, 1H), 2.57-2.41 (m, 4H), 2.23-2.17 (m, 4H), 1.94-1.87 (m, 2H), 1.82-1.72 (m, 2H).

4.6.1.5.

9-(3,5-Dibromo-4-hydroxyphenyl)-3,3,6,6-tetramethyl-3,4,6,7,9,10-hexahydroacridine-1,8(2H,5H)-dione (**4e**)

Compound **4e** was prepared using 3,5-dibromo-4-hydroxybenzaldehyde (280 mg, 1 mmol, 1.0 eq), 5,5-dimethyl-1,3-cyclohexanedione (280 mg, 2 mmol, 2.0 eq) and ammonium acetate (231 mg, 3 mmol, 3.0 eq) according to the general procedure A to give the desired product (458 mg, yield 87.5%) as a yellow solid. ¹H NMR (400 MHz, DMSO-*d*₆) δ 9.38 (s, 1H), 7.21 (s, 2H), 4.67 (s, 1H), 2.45 (d, *J* = 17.1 Hz, 2H), 2.35 (d, *J* = 17.1 Hz, 2H), 2.19 (d, *J* = 16.2 Hz, 2H), 2.01 (d, *J* = 16.2 Hz, 2H), 1.01 (s, 6H), 0.89 (s, 6H).

4.6.2. General procedure B for synthesis of hexahydroquinoline intermediates (**8a-8b**)

To a solution of the 4-hydroxybenzaldehyde (2d, 4 mmol) in THF (10 mL) was added 1,3-cyclohexanedione/5,5-dimethyl-1,3-cyclohexanedione (4 mmol) followed by 3 drops of piperidine. The mixture was stirred at reflux under nitrogen atmosphere for 4 h. The solvent was concentrated in vacuo, and the residue was dissolved in ethanol (10 mL). 3-Aminocrotono-analogue (**7a-7b**, 4 mmol) was added to the solution, and the reaction mixture was stirred at reflux under nitrogen overnight. The resulting precipitate was filtered off and washed with ethanol before drying to afford the desired compounds. The crude product was pure enough to be used without further purification [34].

4.6.2.1. 4-(4-Hydroxyphenyl)-2-methyl-5-oxo-1,4,5,6,7,8-hexahydroquinoline-3-carbonitrile (**8a**)

Compound **8a** was prepared using 4-hydroxybenzaldehyde (488 mg, 4 mmol, 1.0 eq), 1,3-cyclohexanedione (448 mg, 4 mmol, 1.0 eq) and (*E*)-3-aminobut-2-enenitrile (328 mg, 4 mmol, 1.0 eq) according to the general procedure B to give the desired product (472 mg, yield 42.1%) as an off-white solid. ¹H NMR (400 MHz, DMSO-*d*₆) δ 9.46 (s, 1H), 9.26 (s, 1H), 6.98 (d, *J* = 8.5 Hz, 2H), 6.68 (d, *J* = 8.5 Hz, 2H), 4.34 (s, 1H), 2.54 – 2.47 (m, 2H), 2.25- 2.18 (m, 2H), 2.06 (s, 3H), 1.96-1.89 (m, 1H), 1.86-1.76 (m, 1H).

4.6.2.2. Methyl

4-(4-hydroxyphenyl)-2,7,7-trimethyl-5-oxo-1,4,5,6,7,8-hexahydroquinoline-3-carboxylate (**8b**)

Compound **8b** was prepared using 4-hydroxybenzaldehyde (488 mg, 4 mmol, 1.0 eq), 5,5-dimethyl-1,3-cyclohexanedione (560 mg, 4 mmol, 1.0 eq) and methyl (*E*)-3-aminobut-2-enoate (460 mg, 4 mmol, 1.0 eq) according to the general procedure B to give the desired product (480 mg, yield 35.2%) as an off-white solid. ¹H NMR (400 MHz, DMSO-*d*₆) δ 9.06 (s, 1H), 9.02 (s, 1H), 6.91 (d, *J* = 8.5 Hz, 2H), 6.55 (d, *J* = 8.5 Hz, 2H), 4.74 (s, 1H), 3.52 (s, 3H), 2.40 (d, *J* = 17.0 Hz, 1H), 2.26 (s, 3H), 2.25(d, *J* = 17.0 Hz, 1H) , 2.15 (d, *J* = 16.1 Hz, 1H), 1.96 (d, *J* = 16.1 Hz, 1H), 1.00 (s, 3H), 0.84 (s, 3H).

4.6.2.3. Synthesis of naphthalene-acridone intermediate **8c**

A mixture of α-naphthylamine (286 mg, 2 mmol, 1.0 eq), 1,3-cyclohexanedione (224 mg, 2 mmol, 1.0 eq) and 4-hydroxybenzaldehyde (244 mg, 2 mmol, 1.0 eq) in 20 mL of butanol was heated at reflux under

nitrogen atmosphere for 6 h. The precipitate was filtered off and washed with ethanol before drying to afford the desired compound **8c** [29]. ¹H NMR (400 MHz, DMSO-*d*₆) δ 9.26 (s, 1H), 9.07 (s, 1H), 8.45 (d, *J* = 8.4 Hz, 1H), 7.81 (d, *J* = 8.4 Hz, 1H), 7.56 (ddd, *J* = 8.4, 6.8, 1.4 Hz, 1H), 7.51 – 7.47 (m, 1H), 7.45 (d, *J* = 8.4 Hz, 1H), 7.27 (d, *J* = 8.4 Hz, 1H), 7.01 – 6.95 (m, 2H), 6.58 – 6.51 (m, 2H), 5.11 (s, 1H), 2.94-2.85 (m, 1H), 2.73-2.63 (m, 1H), 2.33-2.18 (m, 2H), 2.03-1.95 (m, 1H), 1.93 – 1.83 (m, 1H).

4.6.3. General procedure C for synthesis of target compounds **6a-6h**, **9a-9c**

Potassium hydroxide (6 eq) was ground in a mortar until powdered, then added to a 25 mL Erlenmeyer flask containing 5 mL of dimethyl sulfoxide. The resulting mixture was stirred for 5 min, after which time 1 eq of phenolic hydroxyl intermediates **4a-4f**, **8a-8c** was added. The mixture was stirred an additional 15 min, after which time 1 eq of benzyl bromide derivatives **5a-5c** was added. The reaction was stirred at room temperature for about 4h. Distilled water was added to the brown reaction mixture, and concentrated aqueous hydrochloric acid was added until the pH of the solution was about 5. The mixture was diluted with EtOAc and the aqueous layer was separated and extracted with EtOAc. The organic layers were combined, washed with brine, dried over Na₂SO₄ and concentrated under reduced pressure. The residue was purified by flash column chromatography to give the target compounds.

4.6.3.1.

4-((2,6-Dichloro-4-(1,8-dioxo-1,2,3,4,5,6,7,8,9,10-decahydroacridin-9-yl)phenoxy)methyl)benzoic acid (**6a**)

Compound **6a** was prepared from **4a** (189 mg, 0.5 mmol, 1.0 eq) and 4-(bromomethyl)benzoic acid (**5a**, 108 mg, 0.5 mmol, 1.0 eq) following the general procedure C to give the target product (106 mg, yield 41.3%) as an off-white solid. ¹H NMR (400 MHz, DMSO-*d*₆) δ 13.01 (s, 1H), 9.59 (s, 1H), 7.98 (d, *J* = 8.2 Hz, 2H), 7.62 (d, *J* = 8.2 Hz, 2H), 7.19 (s, 2H), 5.01 (s, 2H), 4.86 (s, 1H), 2.63-2.46 (m, 4H), 2.29-2.16 (m, 4H), 1.97-1.87 (m, 2H), 1.87-1.74 (m, 2H); ¹³C NMR (126 MHz, DMSO-*d*₆) δ 194.90, 167.02, 152.06, 148.01, 145.61, 141.10, 130.53, 129.42, 128.04, 127.97, 127.78, 111.20, 73.87, 36.62, 32.30, 26.28, 20.75; UPLC-MS *m/z* (ESI, positive) found [M+H]⁺ 512.28, >99% pure.

4.6.3.2.

4-((4-(1,8-Dioxo-1,2,3,4,5,6,7,8,9,10-decahydroacridin-9-yl)-2-methoxyphenoxy)methyl)benzoic acid (**6b**)

Compound **6b** was prepared from **4b** (170 mg, 0.5 mmol, 1.0 eq) and 4-(bromomethyl)benzoic acid (**5a**, 108 mg, 0.5 mmol, 1.0 eq) following the general procedure C to give the target product (84 mg, yield 35.6%) as an off-white solid. ¹H NMR (400 MHz, DMSO-*d*₆) δ 12.97 (s, 1H), 9.43 (s, 1H), 7.95 (d, *J* = 8.3, 2H), 7.52 (d, *J* = 8.3 Hz, 2H), 6.84 (d, *J* = 2.0 Hz, 1H), 6.79 (d, *J* = 8.4 Hz, 1H), 6.57 (dd, *J* = 8.4, 2.0 Hz, 1H), 5.07 (s, 2H), 4.88 (s, 1H), 3.70 (s, 3H), 2.51 – 2.41 (m, 4H), 2.24-2.19 (m, 4H), 1.95-1.87 (m, 2H), 1.85 – 1.72 (m, 2H). ¹³C NMR (126 MHz, DMSO-*d*₆) δ 194.89, 167.10, 151.16, 148.41, 145.62, 142.59, 140.74, 129.44, 127.26, 119.00, 113.50, 112.45, 112.24, 69.46, 55.44, 36.83, 31.36, 26.34, 20.86; UPLC-MS *m/z* (ESI, positive) found [M+H]⁺ 474.36, >95% pure.

4.6.3.3.

4-((2-Bromo-4-(3,3,6,6-tetramethyl-1,8-dioxo-1,2,3,4,5,6,7,8,9,10-decahydroacridin-9-yl)phenoxy)methyl)benzoic acid (**6c**)

Compound **6c** was prepared from **4c** (222 mg, 0.5 mmol, 1.0 eq) and 4-(bromomethyl)benzoic acid (**5a**, 108 mg, 0.5 mmol, 1.0 eq) following the general procedure C to give the target product (154 mg, yield 53.1%) as a light-yellow solid. ¹H NMR (400 MHz, DMSO-*d*₆) δ 9.86 (s, 1H), 9.29 (s, 1H), 7.18 (d, *J* = 2.1 Hz, 1H), 6.92 (dd, *J* = 8.3, 2.1 Hz, 1H), 6.74 (d, *J* = 8.3 Hz, 1H), 4.67 (s, 1H), 2.44 (d, *J* = 17.0 Hz, 2H), 2.31 (d, *J* = 17.0 Hz, 2H), 2.17 (d, *J* = 16.1 Hz, 2H), 1.99 (d, *J* = 16.1 Hz, 3H), 1.00 (s, 6H), 0.87 (s,

6H). ^{13}C NMR (126 MHz, DMSO) δ 194.40, 167.07, 152.11, 149.41, 141.77, 141.51, 132.05, 129.44, 127.80, 127.05, 113.44, 111.08, 110.18, 69.41, 54.91, 50.16, 32.17, 29.04, 26.45; UPLC-MS m/z (ESI, positive) found $[\text{M}+\text{H}]^+$ 578.28, >95% pure.

4.6.3.4.

4-((4-(3-Cyano-2-methyl-5-oxo-1,4,5,6,7,8-hexahydroquinolin-4-yl)phenoxy)methyl)benzoic acid (9a)

Compound **9a** was prepared from **8a** (140 mg, 0.5 mmol, 1.0 eq) and 4-(bromomethyl)benzoic acid (**5a**, 108 mg, 0.5 mmol, 1.0 eq) following the general procedure C to give the target product (80 mg, yield 38.7%) as an off-white solid. ^1H NMR (400 MHz, DMSO- d_6) δ 12.97 (s, 1H), 9.48 (s, 1H), 7.95 (d, $J = 8.1$ Hz, 2H), 7.55 (d, $J = 8.1$ Hz, 2H), 7.08 (d, $J = 8.5$ Hz, 2H), 6.92 (d, $J = 8.5$ Hz, 2H), 5.15 (s, 2H), 4.37 (s, 1H), 2.45 – 2.49 (m, 2H), 2.25– 2.16 (m, 2H), 2.04 (s, 3H), 1.95–1.86 (m, 1H), 1.86–1.72 (m, 1H); ^{13}C NMR (126 MHz, DMSO- d_6) δ 194.59, 167.06, 156.86, 151.30, 145.91, 142.30, 138.56, 130.11, 129.47, 128.29, 127.28, 119.89, 114.54, 108.94, 86.05, 68.59, 36.89, 36.63, 26.28, 20.69, 17.60; UPLC-MS m/z (ESI, positive) found $[\text{M}+\text{H}]^+$ 415.34, >99% pure.

4.6.3.5.

4-((4-(3-(Methoxycarbonyl)-2,7,7-trimethyl-5-oxo-1,4,5,6,7,8-hexahydroquinolin-4-yl)phenoxy)methyl)benzoic acid (9b)

Compound **9b** was prepared from **8b** (170 mg, 0.5 mmol, 1.0 eq) and 4-(bromomethyl)benzoic acid (**5a**, 108 mg, 0.5 mmol, 1.0 eq) following the general procedure C to give the target product (60 mg, yield 25.3%) as a yellow solid. ^1H NMR (400 MHz, DMSO- d_6) δ 12.92 (s, 1H), 9.06 (s, 1H), 7.94 (d, $J = 8.3$ Hz, 2H), 7.52 (d, $J = 8.3$ Hz, 2H), 7.05 (d, $J = 8.7$ Hz, 2H), 6.83 (d, $J = 8.7$ Hz, 2H), 5.10 (s, 2H), 4.80 (s, 1H), 3.52 (s, 3H), 3.00 (s, 1H), 2.40 (d, $J = 17.0$ Hz, 1H), 2.27 (s, 3H), 2.26 (d, $J = 17.0$ Hz, 1H), 2.16 (d, $J = 16.1$ Hz, 1H), 1.97 (d, $J = 16.1$ Hz, 1H), 0.99 (s, 3H), 0.83 (s, 3H); ^{13}C NMR (126 MHz, DMSO- d_6) δ 194.27, 167.36, 167.08, 156.25, 149.23, 145.02, 142.30, 140.25, 130.16, 129.41, 128.25, 127.28, 114.05, 110.19, 103.43, 68.52, 50.62, 50.25, 34.73, 32.12, 29.10, 26.49, 18.29; UPLC-MS m/z (ESI, positive) found $[\text{M}+\text{H}]^+$ 476.78, >99% pure.

*4-((4-(8-Oxo-7,8,9,10,11,12-hexahydrobenzo[*c*]acridin-7-yl)phenoxy)methyl)benzoic acid (9c)*

Compound **9c** was prepared from **8c** (170 mg, 0.5 mmol, 1.0 eq) and 4-(bromomethyl)benzoic acid (**5a**, 108 mg, 0.5 mmol, 1.0 eq) following the general procedure C to give the target product (65 mg, yield 27.2%) as a yellow solid. ^1H NMR (400 MHz, DMSO- d_6) δ 12.93 (s, 1H), 9.30 (s, 1H), 8.46 (d, $J = 8.5$ Hz, 1H), 7.96 – 7.88 (m, 2H), 7.86 – 7.78 (m, 1H), 7.61 – 7.53 (m, 1H), 7.53 – 7.43 (m, 4H), 7.28 (d, $J = 8.4$ Hz, 1H), 7.14 – 7.07 (m, 2H), 6.85 – 6.78 (m, 2H), 5.18 (s, 1H), 5.07 (s, 2H), 2.29–2.23 (m, 2H), 2.03–1.96 (m, 3H), 1.94–1.80 (m, 1H); ^{13}C NMR (126 MHz, DMSO- d_6) δ 193.87, 156.28, 153.43, 141.21, 132.23, 130.56, 129.61, 129.39, 128.09, 127.89, 127.14, 125.63, 122.60, 122.13, 121.22, 121.12, 114.36, 108.66, 68.54, 36.77, 31.24, 26.94, 21.04; UPLC-MS m/z (ESI, positive) found $[\text{M}+\text{H}]^+$ 476.32, >99% pure.

4-((2-Bromophenoxy)methyl)benzoic acid (6h)

Compound **6h** was prepared from 2-bromophenol (**4f**, 173 mg, 1 mmol, 1.0 eq) and 4-(bromomethyl)benzoic acid (**5a**, 215 mg, 1 mmol, 1.0 eq) following the general procedure C to give the target product (192 mg, yield 62.5%) as a white solid. ^1H NMR (400 MHz, CDCl_3) δ 8.04 (d, $J = 8.2$ Hz, 2H), 7.54–7.48 (m, 3H), 7.19 (ddd, $J = 8.3, 7.4, 1.6$ Hz, 1H), 6.87 (dd, $J = 8.3, 1.4$ Hz, 1H), 6.81 (td, $J = 7.4, 1.4$ Hz, 1H), 5.16 (s, 2H) (One COOH was not seen); ^{13}C NMR (126 MHz, DMSO- d_6) δ 167.03, 154.20, 141.67, 133.05, 129.49, 128.98, 127.05, 122.41, 114.24, 111.20, 69.36.

4.6.3.8.

9-(4-(Benzyloxy)-3-bromophenyl)-3,3,6,6-tetramethyl-3,4,6,7,9,10-hexahydroacridine-1,8(2H,5H)-dione (6d)

Compound **6d** was prepared from **4c** (222 mg, 0.5 mmol, 1.0 eq) and benzyl bromide (**5b**, 86 mg, 0.5 mmol, 1.0 eq) following the general procedure C to give the target product (199 mg, yield 74.5%) as a white solid. ¹H NMR (400 MHz, DMSO-*d*₆) δ 9.33 (s, 1H), 7.46 – 7.41 (m, 2H), 7.41 – 7.35 (m, 2H), 7.35 – 7.28 (m, 2H), 7.07 (dd, *J* = 8.5, 2.1 Hz, 1H), 7.01 (d, *J* = 8.5 Hz, 1H), 5.09 (s, 2H), 4.72 (s, 1H), 2.45 (d, *J* = 17.1 Hz, 2H), 2.33 (d, *J* = 17.1 Hz, 2H), 2.17 (d, *J* = 16.2 Hz, 2H), 2.00 (d, *J* = 16.2 Hz, 2H), 1.01 (s, 6H), 0.88 (s, 6H); ¹³C NMR (126 MHz, DMSO-*d*₆) δ 194.40, 152.29, 149.38, 141.31, 136.76, 132.00, 128.40, 127.81, 127.34, 113.38, 111.10, 110.17, 69.93, 50.16, 32.17, 32.06, 29.05, 26.45; UPLC-MS *m/z* (ESI, positive) found [M+H]⁺ 534.34, >99% pure.

4.6.3.9.

9-(3-Bromo-4-((3-fluorobenzyl)oxy)phenyl)-3,4,6,7,9,10-hexahydroacridine-1,8(2H,5H)-dione (6e)

Compound **6e** was prepared from **4d** (194 mg, 0.5 mmol, 1.0 eq) and 1-(bromomethyl)-3-fluorobenzene (**5c**, 95 mg, 0.5 mmol, 1.0 eq) following the general procedure C to give the target product (135 mg, yield 54.3%) as an off-white solid. ¹H NMR (400 MHz, DMSO-*d*₆) δ 9.49 (s, 1H), 7.48-7.40 (m, 1H), 7.32 (d, *J* = 2.1 Hz, 1H), 7.30 – 7.24 (m, 2H), 7.19-7.12 (m, 1H), 7.05 (dd, *J* = 8.5, 2.1 Hz, 1H), 6.97 (d, *J* = 8.5 Hz, 1H), 5.14 (s, 2H), 4.81 (s, 1H), 2.58 – 2.51 (m, 4H), 2.26 – 2.15 (m, 4H), 1.95-1.87 (m, 2H), 1.84-1.70 (m, 2H); ¹³C NMR (126 MHz, DMSO-*d*₆) δ 194.81, 152.09, 151.40, 141.73, 139.78, 131.92, 130.55, 127.69, 123.06, 114.65, 113.87, 113.70, 113.61, 112.07, 110.38, 69.08, 36.70, 31.45, 26.28, 20.80; UPLC-MS *m/z* (ESI, positive) found [M+H]⁺ 496.25, >99% pure.

4.6.3.10.

4-((2,6-Dibromo-4-(3,3,6,6-tetramethyl-1,8-dioxo-1,2,3,4,5,6,7,8,9,10-decahydroacridin-9-yl)p henoxymethyl)benzoic acid (6h)

Compound **6h** was prepared from **4e** (261 mg, 0.5 mmol, 1.0 eq) and 4-(bromomethyl)benzoic acid (**5a**, 108 mg, 0.5 mmol, 1.0 eq) following the general procedure C to give the target product (205 mg, yield 62.5%) as a yellow solid. ¹H NMR (400 MHz, DMSO-*d*₆) δ 13.03 (s, 1H), 9.45 (s, 1H), 7.97 (d, *J* = 8.4 Hz, 2H), 7.63 (d, *J* = 8.4 Hz, 2H), 7.36 (s, 2H), 4.99 (s, 2H), 4.76 (s, 1H), 2.45 (d, *J* = 17.1 Hz, 2H), 2.35 (d, *J* = 17.1 Hz, 2H), 2.19 (d, *J* = 16.2 Hz, 2H), 2.01 (d, *J* = 16.2 Hz, 2H), 1.01 (s, 6H), 0.89 (s, 6H); ¹³C NMR (126 MHz, DMSO-*d*₆) δ 194.50, 167.03, 150.01, 149.58, 146.42, 140.98, 131.83, 130.53, 129.38, 127.84, 116.95, 110.33, 73.49, 50.04, 32.72, 32.23, 28.97, 26.39; UPLC-MS *m/z* (ESI, positive) found [M+H]⁺ 656.28, >99% pure.

4.7. Molecular docking

The molecular docking was carried out using the Glide program in Maestro v9.2. The crystal structure of yGCN5 (PDB 1YGH) was used as target for docking. The protein was optimized by the Protein preparation Wizard module in Maestro. A receptor grid box was defined as a 30 Å × 30 Å × 30 Å space region centered on E173. The ligands were prepared by LigPrep module in Maestro v9.2 for the generation of all stereo isomers and different protonation states. Extra-precision (XP) mode was used to perform the molecular docking. The final pose for ligand was selected according to the Glide scoring function (G-Score).

4.8. Cell proliferation assays

MV4-11 cell lines were purchased from ATCC and were maintained in RPMI-1640 medium (Life Technologies) supplemented with 10% FBS and 1% PS (Life Technologies). The cells were cultured in a humidified atmosphere at 37 °C with 5% CO₂ in a CO₂ incubator. For cell proliferation assay, the cells were plated in 96-well plate (Corning) in total volume of 100 µL at a density of 10⁴/well and then treated with compounds dissolved in DMSO at indicated concentration for 72 h. CellTiter-Glo luminescent assays (Promega) were used to determine the fraction of viable cells according to the manufacturer's instruction. The plates were read on a multilabel reader (Envision, PerkinElmer). All treatments were performed in triplicate. All data were analyzed in Graphpad Prism 6.0.

4.9. Cell cycle and Apoptosis assay

For 24 h cell cycle analysis, cells were seeded in 6-well plate (Corning) at a density of 5×10⁵/mL and treated with indicated concentration of compounds or DMSO. After 24 h, cells were harvested and washed three times by 1 mL PBS. Then 70 % (v/v) ethanol was used to re-suspend and fix the sample at 4 °C overnight. Afterwards, the cells were washed twice by PBS again to remove ethanol and stained by PI/Rnase Staining Buffer (BD Pharmingen) at room temperature for further analysis. For 72 h apoptosis assay, the cells were cultured in 6-well plate and treated with compounds as mentioned above. After 72 h incubation, the cells were collected and apoptosis was measured using Annexin V-FITC Apoptosis Detection Kit (Vazyme Biotech) as the manufacturer instructed. All samples were measured by flow cytometry using a LSR II cytometer (BD Pharmingen).

4.10. Western blot

For 24 h acetylation pattern analysis, the cells were cultured in 6-well plate and treated with indicated concentration of compounds or DMSO. 20 µM SAHA was added to each well before compound treatment. After 24 h, the cells were harvested and lysed in 1XSDS cell lysis buffer and boiled for 10 min. Protein samples were subjected to 4%-16% SDS-polyacrylamide gradient gel and transferred to nitrocellulose membranes. The membranes were blocked in 5% (w/v) no fat dry milk for 1 h and incubated with primary antibody at 4 °C overnight. Then the membranes were washed three times by TBST at room temperature. The blots were probed by HRP-conjugated anti-rabbit or anti-mouse IgG antibody and detected by chemiluminescent HRP substrate.

SUPPLEMENTARY MATERIAL

Details on additional experimental procedures, synthesis description, Figures S1-S3 and Table S1. This material is available free of charge via the Internet at <http://pubs.acs.org>.

AUTHOR INFORMATION

Corresponding Author

clu@sim.ac.cn; zhoubing@sim.ac.cn; wclu@shu.edu.cn.

Notes

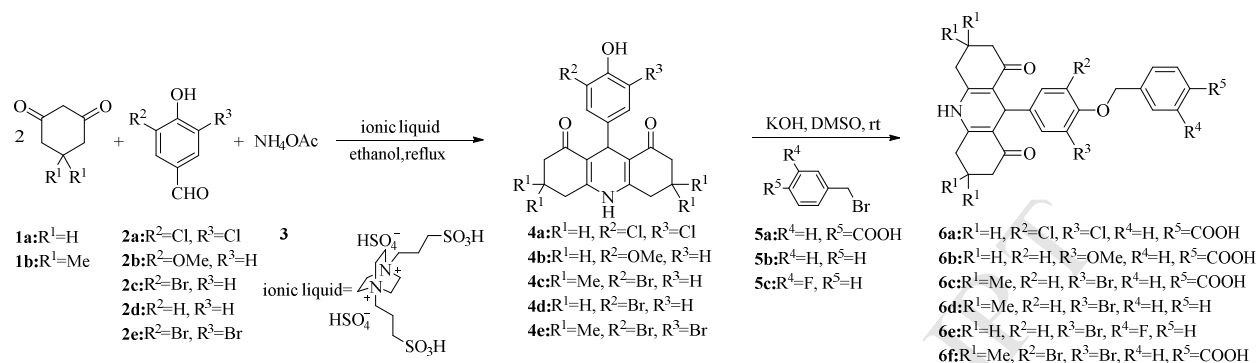
The authors declare no competing financial interests.

ACKNOWLEDGMENT

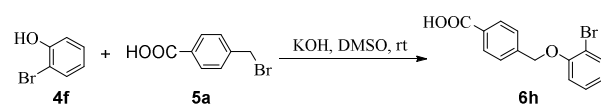
We gratefully acknowledge financial support from the National Natural Science Foundation of China (81625022, 21472208 and 81430084 to C.L.)

ACCEPTED MANUSCRIPT

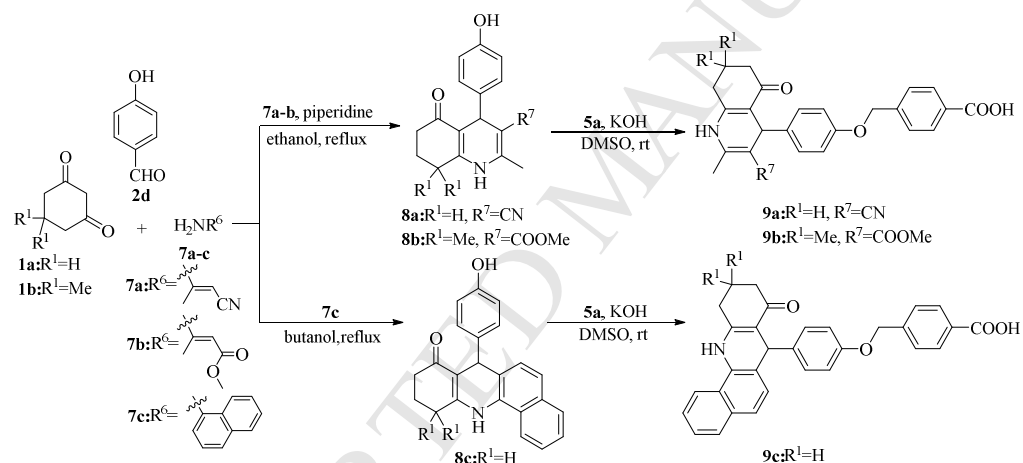
Figures and tables



Scheme 1. Synthesis of 1,8-acridinedione derivatives.

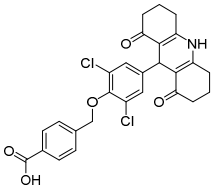
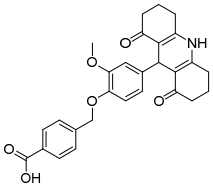
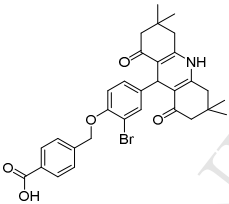
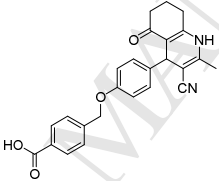
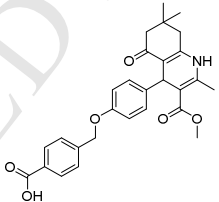
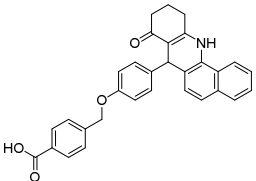
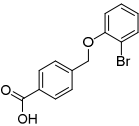
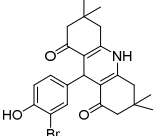


Scheme 2. Synthesis of compound 6h.



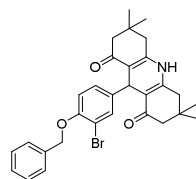
Scheme 3. Synthesis of hexahydroquinoline derivatives.

Table 1: Structures and radioisotope activity for synthesized derivatives

Entry	Compound	Structure	IC ₅₀ (μM)
1	6a (DC_G16)		34.7
2	6b		24%@33 μM
3	6c		16
4	9a		34%@33 μM
5	9b		31
6	9c		34
7	6h		81
8	4c		18%@33 μM

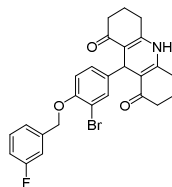
9

6d

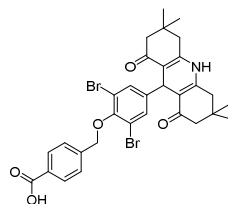
15% @ 33 μ M

10

6e

26% @ 33 μ M

11

6f
(DC_G16-11)

6.8

ACCEPTED MANUSCRIPT

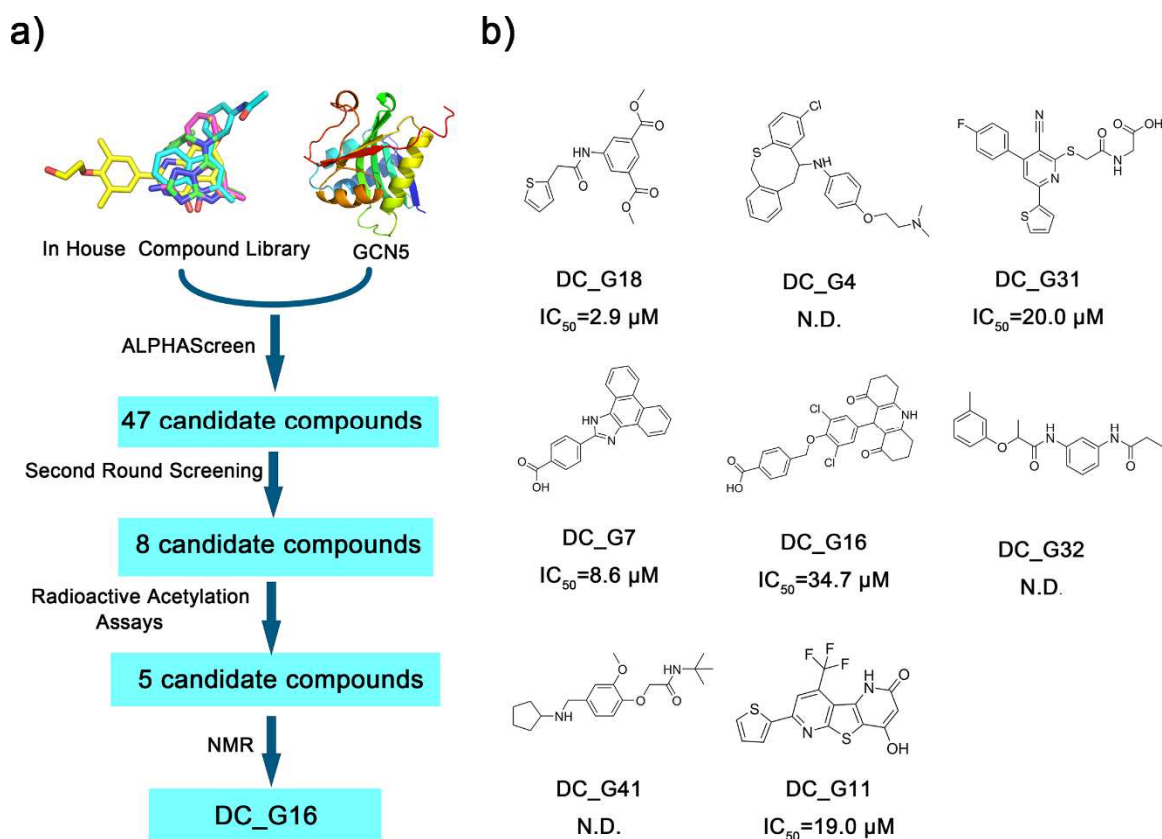


Figure 1. ALPHAScreen-based high throughput screening procedures and GCN5 radioactive acetylation assays results. a) Flowchart of hierarchical high throughput screening for GCN5 inhibitors. b) Inhibitory activities of eight potential hit compounds determined by radioactive acetylation assays.

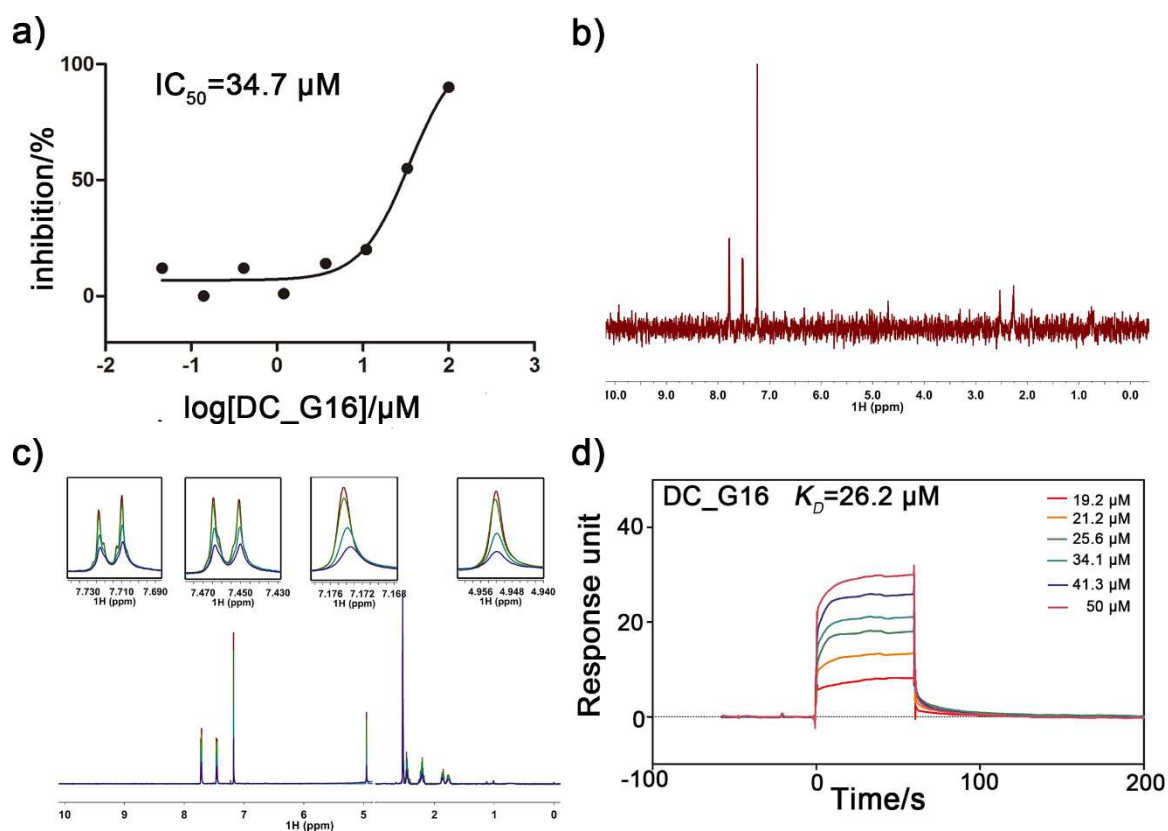


Figure 2. Evaluation of hit compound DC_G16 by biochemical and biophysical assays *in vitro*. a) The inhibitory activity of **DC_G16** determined in GCN5 radioisotope assay. b) STD NMR experiments of 5 μM GCN5 in the presence of 200 μM **DC_G16**. c) Dose-dependent CPMG spectra for 200 μM **DC_G16** (red) in the presence of 5 μM GCN5 (blue), 2 μM GCN5 (green) and 1 μM GCN5 (aqua). d) SPR-based binding assay of **DC_G16** with GCN5. The compound was prepared at concentration of 19.2 μM , 21.2 μM , 25.6 μM , 34.1 μM , 41.3 μM , and 50 μM , respectively.

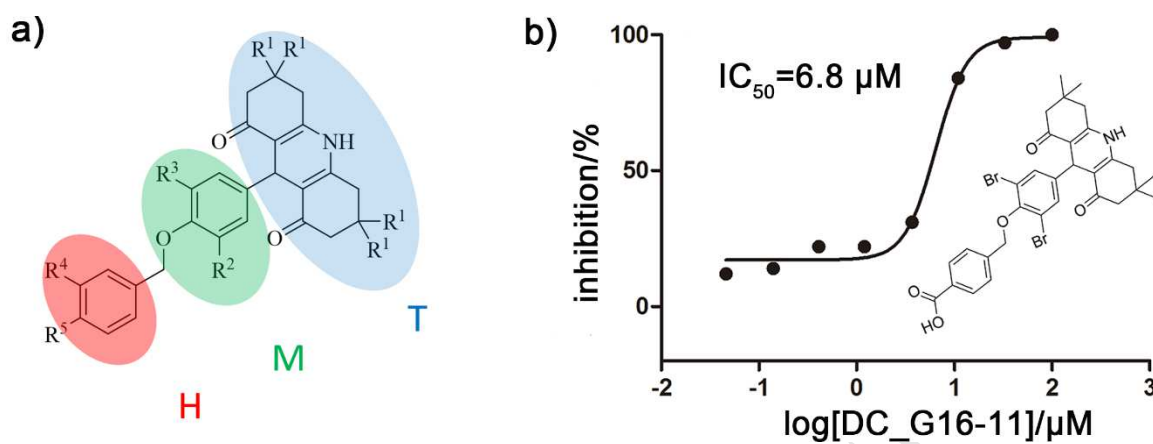


Figure 3. a) Decomposition diagrams of 1,8-acridinedione scaffold. The scaffold was divided into three parts: H (head region), M (middle region) and T (tail region) which were highlighted in red, green and blue ellipses, respectively. b) The structure and inhibitory activity against GCN5 of DC_G16-11 based on acetylation assay.

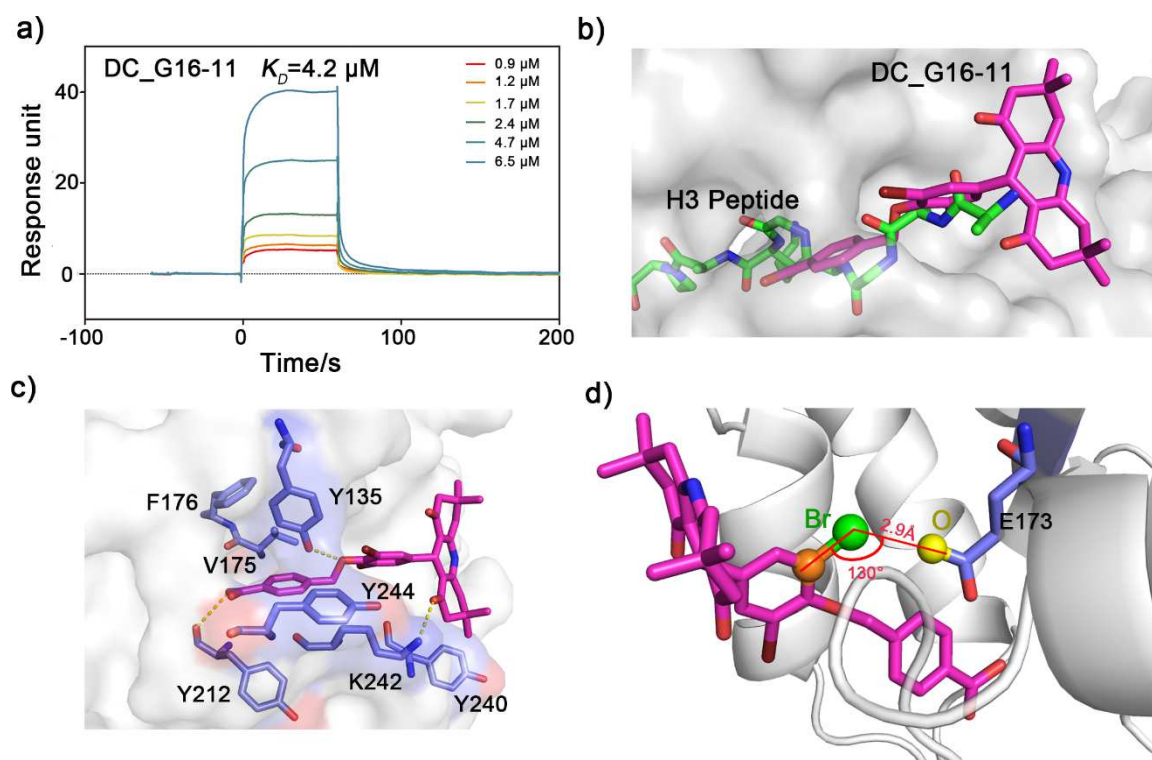


Figure 4. The interaction and putative binding mode between DC_G16-11 and GCN5. a) SPR based binding assay of DC_G16-11 with GCN5. The compound was prepared at concentration of 0.9 μM , 1.2 μM , 1.7 μM , 2.4 μM , 4.7 μM and 6.5 μM , respectively. b) The alignment of H3 peptide binding site of tetrahymena GCN5 (PDB ID: 1QSN) and predicted binding conformation of DC_G16-11. H3 peptide is depicted as green sticks, while DC_G16-11 is depicted as magenta sticks. GCN5 is shown in white surface. c) Close-up view of the key interactions stabilizing DC_G16-11 in H3 peptide binding pocket. DC_G16-11 is depicted as magenta sticks, the surrounding key residues are shown in slate sticks and labelled. Hydrogen bonds are shown as yellow dot lines. GCN5 is shown in white surface. d) A putative halogen bond between bromine atom and oxygen atom. Bromine atom, oxygen atom and carbon atom involved in halogen bond are shown in green, yellow and orange ball, respectively, the measurement results of distance between Br and O and angle of C–Br...O are shown in red. DC_G16-11 is depicted as magenta sticks. E173 is shown in slate sticks.

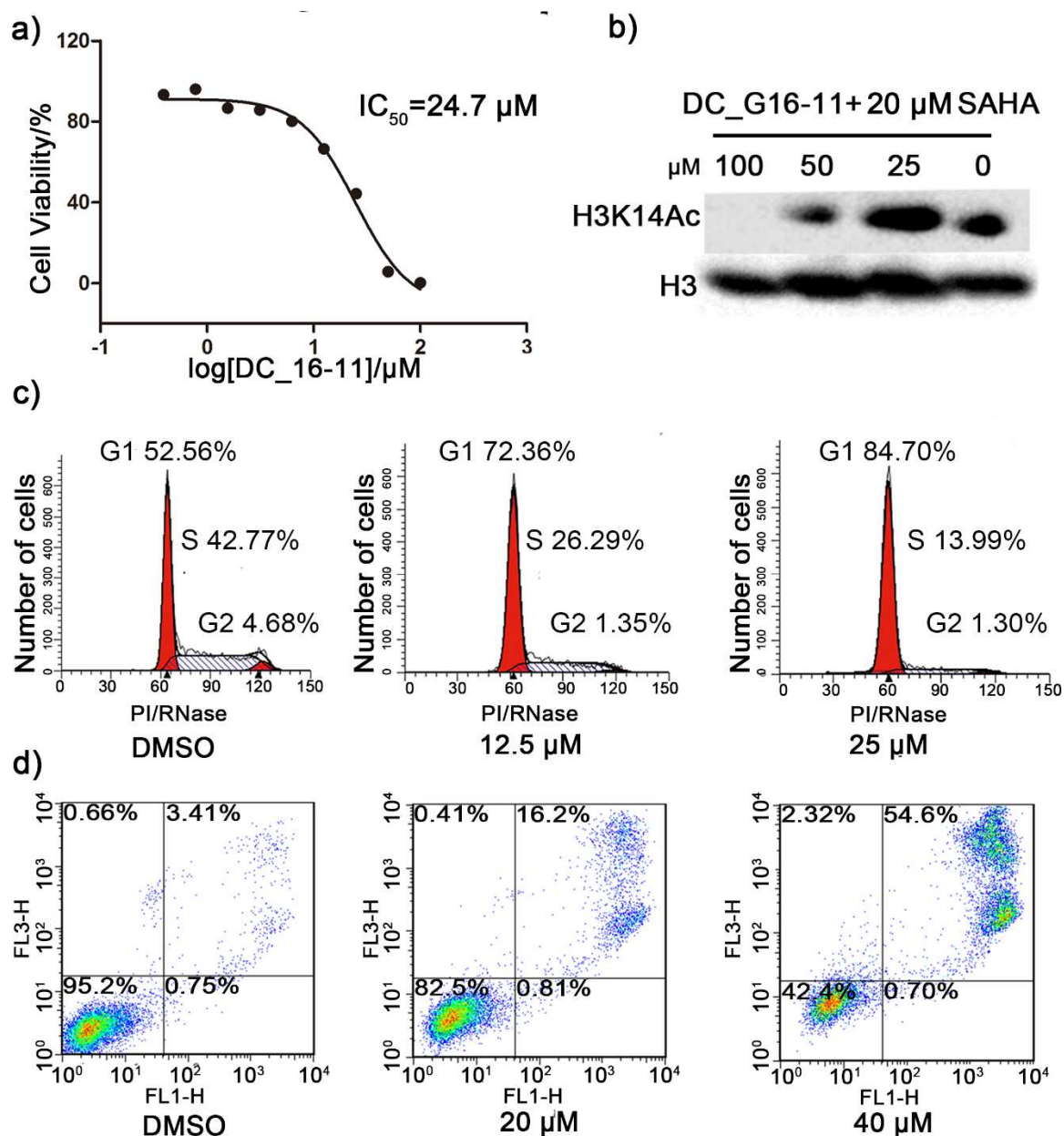


Figure 5. Evaluation of compound DC_G16-11 at cellular level. a) Cell proliferation inhibition assay for DC_G16-11. b) Acetylation pattern analysis of H3K14 by western blot co-treated with 20 μM SAHA. MV4-11 cells were treated with 0 μM , 25 μM , 50 μM and 100 μM DC_G16-11 for 24 h. c) 24 h cell cycle analysis. MV4-11 cells were treated with 0 μM , 12.5 μM and 25 μM DC_G16-11 for 24 h. d) 72 h cell apoptosis analysis. MV4-11 cells were treated with 0 μM , 20 μM and 40 μM DC_G16-11 for 72 h.

Reference

- [1] J.A. Latham, S.Y. Dent, Cross-regulation of histone modifications, *Nat. Struct. Mol. Biol.*, 14 (2007) 1017-1024.
- [2] B.D. Strahl, C.D. Allis, The language of covalent histone modifications, *Nature*, 403 (2000) 41-45.
- [3] C. Choudhary, C. Kumar, F. Gnad, M.L. Nielsen, M. Rehman, T.C. Walther, J.V. Olsen, M. Mann, Lysine acetylation targets protein complexes and co-regulates major cellular functions, *Science*, 325 (2009) 834-840.
- [4] C.H. Arrowsmith, C. Bountra, P.V. Fish, K. Lee, M. Schapira, Epigenetic protein families: a new frontier for drug discovery, *Nat. Rev. Drug Discovery*, 11 (2012) 384-400.
- [5] M.H. Kuo, J.E. Brownell, R.E. Sobel, T.A. Ranalli, R.G. Cook, D.G. Edmondson, S.Y. Roth, C.D. Allis, Transcription-linked acetylation by Gcn5p of histones H3 and H4 at specific lysines, *Nature*, 383 (1996) 269-272.
- [6] P.A. Grant, A. Eberharter, S. John, R.G. Cook, B.M. Turner, J.L. Workman, Expanded lysine acetylation specificity of Gcn5 in native complexes, *J. Biol. Chem.*, 274 (1999) 5895-5900.
- [7] R.L. Schiltz, C.A. Mizzen, A. Vassilev, R.G. Cook, C.D. Allis, Y. Nakatani, Overlapping but distinct patterns of histone acetylation by the human coactivators p300 and PCAF within nucleosomal substrates, *J. Biol. Chem.*, 274 (1999) 1189-1192.
- [8] N.A. Barlev, L. Liu, N.H. Chehab, K. Mansfield, K.G. Harris, T.D. Halazonetis, S.L. Berger, Acetylation of p53 activates transcription through recruitment of coactivators/histone acetyltransferases, *Mol. Cell*, 8 (2001) 1243-1254.
- [9] C. Lerin, J.T. Rodgers, D.E. Kalume, S.H. Kim, A. Pandey, P. Puigserver, GCN5 acetyltransferase complex controls glucose metabolism through transcriptional repression of PGC-1alpha, *Cell Metab.*, 3 (2006) 429-438.
- [10] C.D. Tavares, K. Sharabi, J.E. Dominy, Y. Lee, M. Isasa, J.M. Orozco, M.P. Jedrychowski, T.M. Kamenecka, P.R. Griffin, S.P. Gygi, P. Puigserver, The Methionine Transamination Pathway Controls Hepatic Glucose Metabolism through Regulation of the GCN5 Acetyltransferase and the PGC-1alpha Transcriptional Coactivator, *J. Biol. Chem.*, 291 (2016) 10635-10645.
- [11] L. Howe, D. Auston, P. Grant, S. John, R.G. Cook, J.L. Workman, L. Pillus, Histone H3 specific acetyltransferases are essential for cell cycle progression, *Genes Dev.*, 15 (2001) 3144-3154.
- [12] M. Sakai, T. Tujimura-Hayakawa, T. Yagi, H. Yano, M. Mitsushima, H. Unoki-Kubota, Y. Kaburagi, H. Inoue, Y. Kido, M. Kasuga, M. Matsumoto, The GCN5-CITED2-PKA signalling module controls hepatic glucose metabolism through a cAMP-induced substrate switch, *Nat. Commun.*, 7 (2016) 13147.
- [13] Y.W. Yin, H.J. Jin, W. Zhao, B. Gao, J. Fang, J. Wei, D.D. Zhang, J. Zhang, D. Fang, The Histone Acetyltransferase GCN5 Expression Is Elevated and Regulated by c-Myc and E2F1 Transcription Factors in Human Colon Cancer, *Gene Expression*, 16 (2015) 187-196.
- [14] L. Chen, T. Wei, X. Si, Q. Wang, Y. Li, Y. Leng, A. Deng, J. Chen, G. Wang, S. Zhu, J. Kang, Lysine acetyltransferase GCN5 potentiates the growth of non-small cell lung cancer via promotion of E2F1, cyclin D1, and cyclin E1 expression, *J. Biol. Chem.*, 288 (2013) 14510-14521.

- [15] P. Cheung, K.G. Tanner, W.L. Cheung, P. Sassone-Corsi, J.M. Denu, C.D. Allis, Synergistic coupling of histone H3 phosphorylation and acetylation in response to epidermal growth factor stimulation, *Mol. Cell*, 5 (2000) 905-915.
- [16] T. Holmlund, M.J. Lindberg, D. Grander, A.E. Wallberg, GCN5 acetylates and regulates the stability of the oncoprotein E2A-PBX1 in acute lymphoblastic leukemia, *Leukemia*, 27 (2013) 578-585.
- [17] A.N. Poux, M. Cebrat, C.M. Kim, P.A. Cole, R. Marmorstein, Structure of the GCN5 histone acetyltransferase bound to a bisubstrate inhibitor, *Proc. Natl. Acad. Sci. U. S. A.*, 99 (2002) 14065-14070.
- [18] O.D. Lau, T.K. Kundu, R.E. Soccio, S. Ait-Si-Ali, E.M. Khalil, A. Vassilev, A.P. Wolffe, Y. Nakatani, R.G. Roeder, P.A. Cole, HATs off: selective synthetic inhibitors of the histone acetyltransferases p300 and PCAF, *Mol. Cell*, 5 (2000) 589-595.
- [19] F.D. Piazz, A. Vassallo, O.C. Rubio, S. Castellano, G. Sbardella, N. De Tommasi, Chemical biology of histone acetyltransferase natural compounds modulators, *Mol. Diversity*, 15 (2011) 401-416.
- [20] S.D. Furdas, S. Kannan, W. Sippl, M. Jung, Small molecule inhibitors of histone acetyltransferases as epigenetic tools and drug candidates, *Arch. Pharm. (Weinheim, Ger.)*, 345 (2012) 7-21.
- [21] M. Biel, A. Kretsovali, E. Karatzali, J. Papamatheakis, A. Giannis, Design, synthesis, and biological evaluation of a small-molecule inhibitor of the histone acetyltransferase Gcn5, *Angew. Chem.*, 43 (2004) 3974-3976.
- [22] L. Stimson, M.G. Rowlands, Y.M. Newbatt, N.F. Smith, F.I. Raynaud, P. Rogers, V. Bavetsias, S. Gorsuch, M. Jarman, A. Bannister, T. Kouzarides, E. McDonald, P. Workman, G.W. Aherne, Isothiazolones as inhibitors of PCAF and p300 histone acetyltransferase activity, *Mol. Cancer Ther.*, 4 (2005) 1521-1532.
- [23] J.M. Gajer, S.D. Furdas, A. Grunder, M. Gothwal, U. Heinicke, K. Keller, F. Colland, S. Fulda, H.L. Pahl, I. Fichtner, W. Sippl, M. Jung, Histone acetyltransferase inhibitors block neuroblastoma cell growth in vivo, *Oncogenesis*, 4 (2015) e137.
- [24] E.M. Bowers, G. Yan, C. Mukherjee, A. Orry, L. Wang, M.A. Holbert, N.T. Crump, C.A. Hazzalin, G. Liszczak, H. Yuan, C. Larocca, S.A. Saldanha, R. Abagyan, Y. Sun, D.J. Meyers, R. Marmorstein, L.C. Mahadevan, R.M. Alani, P.A. Cole, Virtual ligand screening of the p300/CBP histone acetyltransferase: identification of a selective small molecule inhibitor, *Chem. Biol. (Oxford, U. K.)*, 17 (2010) 471-482.
- [25] L.M. Lasko, C.G. Jakob, R.P. Edalji, W. Qiu, D. Montgomery, E.L. Digiammarino, T.M. Hansen, R.M. Risi, R. Frey, V. Manaves, B. Shaw, M. Algire, P. Hessler, L.T. Lam, T. Uziel, E. Faivre, D. Ferguson, F.G. Buchanan, R.L. Martin, M. Torrent, G.G. Chiang, K. Karukurichi, J.W. Langston, B.T. Weinert, C. Choudhary, P. de Vries, J.H. Van Drie, D. McElligott, E. Kesicki, R. Marmorstein, C. Sun, P.A. Cole, S.H. Rosenberg, M.R. Michaelides, A. Lai, K.D. Bromberg, Discovery of a selective catalytic p300/CBP inhibitor that targets lineage-specific tumours, *Nature*, 550 (2017) 128-132.
- [26] R. Macarron, M.N. Banks, D. Bojanic, D.J. Burns, D.A. Cirovic, T. Garyantes, D.V. Green, R.P. Hertzberg, W.P. Janzen, J.W. Paslay, U. Schopfer, G.S. Sittampalam, Impact of high-throughput screening in biomedical research, *Nat. Rev. Drug Discovery*, 10 (2011) 188-195.

- [27] J. Xing, W. Lu, R. Liu, Y. Wang, Y. Xie, H. Zhang, Z. Shi, H. Jiang, Y.C. Liu, K. Chen, H. Jiang, C. Luo, M. Zheng, Machine-Learning-Assisted Approach for Discovering Novel Inhibitors Targeting Bromodomain-Containing Protein 4, *J. Chem. Inf. Model.*, 57 (2017) 1677-1690.
- [28] Erratum: Borderud SP, Li Y, Burkhalter JE, Sheffer CE and Ostroff JS. Electronic cigarette use among patients with cancer: Characteristics of electronic cigarette users and their smoking cessation outcomes. *Cancer*. doi: 10.1002/ cncr.28811, *Cancer*, 121 (2015) 800.
- [29] V. Nadaraj, S.T. Selvi, S. Mohan, Microwave-induced synthesis and anti-microbial activities of 7,10,11,12-tetrahydrobenzo[c]acridin-8(9H)-one derivatives, *Eur. J. Med. Chem.*, 44 (2009) 976-980.
- [30] R. Wilcken, M.O. Zimmermann, A. Lange, A.C. Joerger, F.M. Boeckler, Principles and applications of halogen bonding in medicinal chemistry and chemical biology, *J. Med. Chem.*, 56 (2013) 1363-1388.
- [31] W.Y. Zhang, W.C. Lu, H. Jiang, Z.B. Lv, Y.Q. Xie, F.L. Lian, Z.J. Liang, Y.X. Jiang, D.J. Wang, C. Luo, J. Jin, F. Ye, Discovery of alkyl bis(oxy)dibenzimidamide derivatives as novel protein arginine methyltransferase 1 (PRMT1) inhibitors, *Chem. Biol. Drug Des.*, 90 (2017) 1260-1270.
- [32] S. Chen, Y. Wang, W. Zhou, S. Li, J. Peng, Z. Shi, J. Hu, Y.C. Liu, H. Ding, Y. Lin, L. Li, S. Cheng, J. Liu, T. Lu, H. Jiang, B. Liu, M. Zheng, C. Luo, Identifying novel selective non-nucleoside DNA methyltransferase 1 inhibitors through docking-based virtual screening, *J. Med. Chem.*, 57 (2014) 9028-9041.
- [33] R.D. Bland, T.L. Clarke, L.B. Harden, Rapid infusion of sodium bicarbonate and albumin into high-risk premature infants soon after birth: a controlled, prospective trial, *Am. J. Obstet. Gynecol.*, 124 (1976) 263-267.
- [34] G.B. Arhancet, S.S. Woodard, K. Iyanar, B.L. Case, R. Woerndle, J.D. Dietz, D.J. Garland, J.T. Collins, M.A. Payne, J.R. Blinn, S.I. Pomposiello, X. Hu, M.I. Heron, H.C. Huang, L.F. Lee, Discovery of novel cyanodihydropyridines as potent mineralocorticoid receptor antagonists, *J. Med. Chem.*, 53 (2010) 5970-5978.